

Non-singular cloaks allow mimesis

André Diatta ^{1*} and Sébastien Guenneau ²

April 21, 2022

^{1*}University of Liverpool. Department of Mathematical Sciences,
M.O. Building, Peach Street, Liverpool L69 3BX, UK

Email address: adiatta@liv.ac.uk;

²Institut Fresnel-CNRS (UMR 6133), University of Aix-Marseille,
case 162, F13397 Marseille Cedex 20, France.

Email address: sebastien.guenneau@fresnel.fr; guenneau@liv.ac.uk

Abstract

We design non-singular cloaks enabling objects to scatter waves like objects with smaller size and very different shapes. We consider the Schrödinger equation which is valid e.g. in the contexts of geometrical and quantum optics. More precisely, we introduce a generalized non-singular transformation for star domains, and numerically demonstrate that an object of nearly any given shape surrounded by a given cloak scatters waves in exactly the same way as a smaller object of another shape. When a source is located inside the cloak, it scatters waves as if it would be located some distance away from a small object. Moreover, the invisibility region actually hosts almost-trapped eigenstates. Mimeticism is numerically shown to break down for the quantified energies associated with confined modes. If we further allow for non-isomorphic transformations, our approach leads to the design of quantum super-scatterers: a small size object surrounded by a quantum cloak described by a negative anisotropic heterogeneous effective mass and a negative spatially varying potential scatters matter waves like a larger nano-object of different shape. Potential applications might be for instance in quantum dots probing. The results within this paper as well as the corresponding derived constitutive tensors, are valid for cloaks with any arbitrary star shaped boundaries cross sections, although for numerical simulations, we use examples with piecewise linear or elliptic boundaries.

1 Introduction

Control of electromagnetic waves can be achieved through coordinate transformations which bring exotic material parameters [1, 2, 3]. Electromagnetic metamaterials within which negative refraction and focussing effects involving the near field can occur [4, 6, 7, 8] can be understood in light of transformation optics [3].

Recently, an electron focussing effect across a p-n junction in a Graphene film, that mimics the Pendry-Veselago lens in optics has been proposed [9]. The subsequent theoretical demonstration of 100 per cent transmission of cold rubidium atom through an array of sub de Broglie wavelength slits, brings the original continuous wave phenomenon in contact with the quantum world [10].

Other types of waves such as water waves can be controlled in a similar way using transformation acoustics [11], leading to invisibility cloaks for pressure waves thanks to the design of two-dimensional [12, 13] and three-dimensional cloaks [14, 15]. It has been further demonstrated that broadband cloaking of surface water waves can be achieved with a structured cloak [16]. Interestingly, cloaking can be further extended to in-plane elastic waves [11, 17] and bending waves in thin-plates [18].

In this paper, we focus our analysis on cloaking of quantum waves which involves spatially varying potentials and anisotropic effective mass of particles, as first proposed by the team of Zhang [19] and further mathematically studied by Greenleaf et al. [20]. We build up on the former proposal to render a quantum object smaller, larger, or even change its shape. Our point here is to apply the versatile tool of transformation physics in an area where the size of the object might have some dramatic changes in the physics: for instance, a quantum super-scatterer might enhance the interactions of quantum dots with the mesoscopic scale, thereby enabling quantum effects in metamaterials.

2 Transformed governing equations for matter waves

Following the proposal by Zhang et al. [19], we consider electrons in a crystal with slowly varying composition: $V = E_b + U$ is the spatially varying potential, E_b the energy of the local band edge and U a slowly varying external potential. In cylindrical coordinates with z invariance, and letting the mass density m_0 be isotropic diagonal in these coordinates, the time independent Schrödinger equation takes the form

$$-\frac{\hbar}{2}\nabla \cdot (m_0^{-1}\nabla\Psi) + V\Psi = E\Psi. \quad (1)$$

Here, \hbar is the Plank constant and Ψ is the wave function. Importantly, this equation is supplied with Neumann boundary conditions on the boundary of the object to be cloaked. Let us consider a map from a co-ordinate system $\{u, v, w\}$ to the co-ordinate system $\{x, y, z\}$ given by the transformation characterized by $x(u, v, w)$, $y(u, v, w)$ and $z(u, v, w)$. This change of co-ordinates is characterized by the transformation of the differentials through the Jacobian:

$$\begin{pmatrix} dx \\ dy \\ dz \end{pmatrix} = \mathbf{J}_{xu} \begin{pmatrix} du \\ dv \\ dw \end{pmatrix}, \text{ with } \mathbf{J}_{xu} = \frac{\partial(x, y, z)}{\partial(u, v, w)}. \quad (2)$$

On a geometric point of view, the matrix $\mathbf{T} = \mathbf{J}^T \mathbf{J} / \det(\mathbf{J})$ is a representation of the metric tensor. The only thing to do in the transformed coordinates is to replace the effective mass (homogeneous and isotropic) and potential by equivalent ones. The effective mass

becomes heterogeneous and anisotropic, while the potential gets a new expression. Their properties are given by [19]

$$\underline{\underline{m}}' = m_0 \mathbf{T}_T^{-1}, \quad V' = E + T_{zz}^{-1}(V - E), \quad (3)$$

where \mathbf{T}_T^{-1} stands for the upper diagonal part of the inverse of \mathbf{T} and T_{zz} is the third diagonal entry of \mathbf{T} .

The transformed equation associated with the quantum mechanical scattering problem (1) reads

$$-\frac{\hbar}{2} \nabla \cdot \underline{\underline{m}}'^{-1} \nabla \Psi + V' \Psi = E \Psi, \quad (4)$$

where importantly the energy E remains unchanged and the wave function $\Psi(x, y) = \exp(i\sqrt{E}(xk_1 + yk_2)) + \Psi_d(x, y)$ with $\sqrt{k_1^2 + k_2^2} = 1$. We note that Ψ_d satisfies the usual Sommerfeld radiation condition (also known as outgoing wave condition in the context of electromagnetic and acoustic waves) which ensures the existence and uniqueness of the solution to (4).

It is indeed the potential V' and the mass density tensor $\underline{\underline{m}}'$ (e.g. involving ultra-cold atoms trapped in an optical lattice as proposed in [19]) which play the role of the quantum cloak at a given energy E . However, there is a simple correspondence between the Schrödinger equation and the Helmholtz equation, the energy E of the former being related to the wave frequency ω of the latter via $\omega = \sqrt{E}$ (up to the normalization $c = \sqrt{2}/\sqrt{\hbar}$, with c the wavespeed in the background medium, say vacuum). The present analysis thus covers cloaking of acoustic and electromagnetic waves governed by a Helmholtz equation. Correspondences bridging the current analysis with a model of transverse electric waves in cylindrical metamaterials are $\underline{\underline{m}}' \longleftrightarrow \underline{\underline{\epsilon}}'$ on the one hand and $\sqrt{V' - E} \longleftrightarrow \omega$ on the other hand.

3 Mathematical setup: Generalized cloaks for star domains

This section is dedicated to a mathematical model generalizing the blowup of a point to a transformation sending a domain to another, thus making the latter inherit the same electronic, electromagnetic or acoustic behavior as the former, depending upon the physical context. Although in this paper we will restrict ourselves to cloaking regions in the plane or 3D Euclidean space, the transformation we propose can be readily extended to any star domain in \mathbb{R}^n , that is, domains with a vantage point from which all points are within line-of-sight. In particular, the transformation still preserves all lines passing through that chosen fixed point.

Here is a description of the transformation in layman terms, but this could be formalised mutatis mutandis in very abstract mathematical settings by working directly with the divergence-form PDE of electrostatics [21] or as the Laplace-Beltrami equation of an associated Riemannian metric [22]. For simplicity, let us consider bounded star domains D_j in \mathbb{R}^n , $n = 2, 3$ with piecewise smooth arbitrary boundaries ∂D_j , all sharing the same chosen vantage point, $j = 0, 1, 2$. We suppose D_2 contains D_1 which in turn, contains D_0 .

Typically, D_1 is the domain to be made to mimic D_0 . The new transformation will be the identity outside D_2 , that is, in $\mathbb{R}^n \setminus D_2$, but will send the hollow region $D_2 \setminus D_0$ to the hollow region $D_2 \setminus D_1$, in such a way that the boundary ∂D_2 of D_2 will stay point-wise fixed, while that of D_0 will be mapped to ∂D_1 . The hollow region $D_2 \setminus D_1$ is meant to be the model for the cloak, endowed with Neumann conditions on its inner boundary ∂D_1 , and in which any type of defect could be concealed, but will still have the same electronic (resp. electromagnetic or acoustic) response as the region D_0 with a potential wall (resp. infinitely conducting boundary or rigid obstacle) of boundary ∂D_0 . In practise, we may divide the domains D_j into subdomains, the part of whose boundaries lying inside ∂D_j is a smooth arbitrary hypersurface.

However, in such an ideal cloaking, there is a dichotomy between generic values of the energy E (resp. wave frequency ω), for which the wave function must vanish within the cloaked region $D_1 \setminus D_0$, and the discrete set of Neumann eigenvalues of $D_1 \setminus D_0$, for which there exist trapped states: waves which are zero outside of $D_1 \setminus D_0$ and equal to a Neumann eigenfunction within $D_1 \setminus D_0$. Such trapped modes have been discussed in [22] when D_0 vanishes.

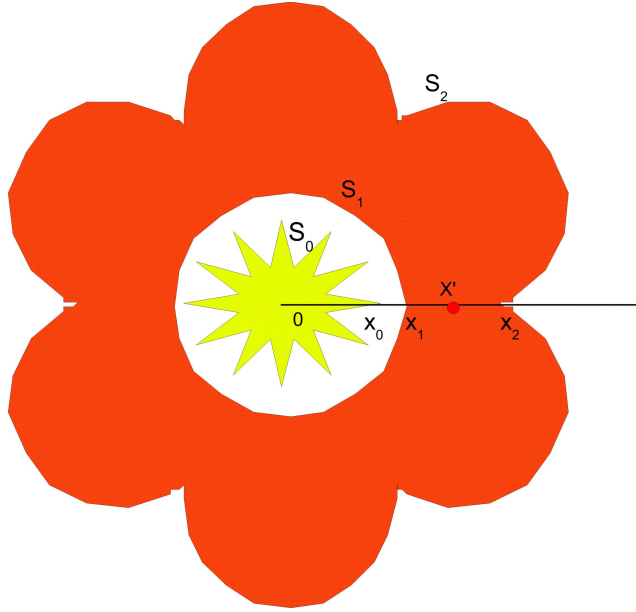


Figure 1: *Construction of a generalized non-singular cloak for mimetism. The transformation with inverse (6) shrinks the region bounded by the two surfaces S_0 and S_2 into the region bounded by S_1 and S_2 . The curvilinear metric inside the carpet (here, an orange flower) is described by the transformation matrix \mathbf{T} , see (7)-(14). This is designed to play the double role of mimesis and cloaking: any types of quantum objects located within the region D_1 bounded by the surface S_1 will be invisible to an outer observer while the region itself still scatters matter waves like an object D_0 bounded by S_0 (here, a yellow star). In the limit of vanishing yellow region, the transformation matrix \mathbf{T} becomes singular on S_1 (ordinary invisibility cloak).*

The transformation is constructed as follows. Consider a point $\underline{\mathbf{x}}$ of $D_1 \setminus D_0$ with $\underline{\mathbf{x}} = (x^1, x^2, \dots)$ relative to a system of coordinates centered at the chosen vantage point $\underline{\mathbf{0}}$. The line passing through $\underline{\mathbf{x}}$ and $\underline{\mathbf{0}}$ meets the boundaries ∂D_0 , ∂D_1 , ∂D_2 at the unique points

$\underline{\mathbf{x}}_0$, $\underline{\mathbf{x}}_1$, $\underline{\mathbf{x}}_2$, respectively. We actually need the inverse $\underline{\mathbf{x}}' \mapsto \underline{\mathbf{x}}$ of the transformation, in the coordinates system, it reads $x^i = x_0^i + \alpha_i (x'^i - x_1^i)$, where $\alpha_i = \frac{x_2^i - x_0^i}{x_2^i - x_1^i}$. In the 3-space with coordinates $(x^1, x^2, x^3) = (x, y, z)$ we can write this transformation as

$$\begin{cases} x = x_0 + \alpha (x' - x_1), & \text{with } \alpha = \frac{x_2 - x_0}{x_2 - x_1} \\ y = y_0 + \beta (y' - y_1) & \text{with } \beta = \frac{y_2 - y_0}{y_2 - y_1} \\ z = z_0 + \gamma (z' - z_1), & \text{with } \gamma = \frac{z_2 - z_0}{z_2 - z_1} \end{cases} \quad (5)$$

The cases of interest in this paper can all be considered as cylinders over some plane curves (triangular, square, elliptic, sun flower-like cylinders, etc.) Thus, we consider the transformation mapping the region enclosed between the cylinders \mathbf{S}_0 and \mathbf{S}_2 into the space between \mathbf{S}_1 and \mathbf{S}_2 as in Figure 1, whose inverse is

$$\begin{cases} x = x_0 + \alpha (x' - x_1), & \text{with } \alpha = \frac{x_2 - x_0}{x_2 - x_1} \\ y = y_0 + \beta (y' - y_1) & \text{with } \beta = \frac{y_2 - y_0}{y_2 - y_1} \\ z = z' \end{cases} \quad (6)$$

The matrix representation of the tensor \mathbf{T}^{-1} is thus given by

$$\mathbf{T}^{-1} = \begin{pmatrix} T_{11}^{-1} & T_{12}^{-1} & 0 \\ T_{12}^{-1} & T_{22}^{-1} & 0 \\ 0 & 0 & T_{33}^{-1} \end{pmatrix} \quad (7)$$

with

$$T_{11}^{-1} = \frac{a_{11}}{a_{33}}, \quad T_{12}^{-1} = \frac{a_{12}}{a_{33}}, \quad T_{22}^{-1} = \frac{a_{22}}{a_{33}}, \quad T_{33}^{-1} = a_{33}, \quad (8)$$

where the coefficients a_{ij} can be expressed as

$$a_{11} = \left(\frac{\partial x}{\partial y'} \right)^2 + \left(\frac{\partial y}{\partial y'} \right)^2, \quad a_{12} = - \left(\frac{\partial x}{\partial x'} \frac{\partial x}{\partial y'} + \frac{\partial y}{\partial x'} \frac{\partial y}{\partial y'} \right), \quad (9)$$

$$a_{22} = \left(\frac{\partial x}{\partial x'} \right)^2 + \left(\frac{\partial y}{\partial x'} \right)^2, \quad a_{33} = \frac{\partial x}{\partial x'} \frac{\partial y}{\partial y'} - \frac{\partial x}{\partial y'} \frac{\partial y}{\partial x'} \quad (10)$$

and finally the partial derivatives are as follows

$$\frac{\partial x}{\partial x'} = \frac{x_2 - x_0}{x_2 - x_1} + \frac{x_2 - x'}{x_2 - x_1} \frac{\partial x_0}{\partial x'} - \frac{(x_2 - x_0)(x_2 - x')}{(x_2 - x_1)^2} \frac{\partial x_1}{\partial x'} - \frac{(x_1 - x_0)(x' - x_1)}{(x_2 - x_1)^2} \frac{\partial x_2}{\partial x'}, \quad (11)$$

$$\frac{\partial x}{\partial y'} = \frac{x_2 - x'}{x_2 - x_1} \frac{\partial x_0}{\partial y'} - \frac{(x_2 - x_0)(x_2 - x')}{(x_2 - x_1)^2} \frac{\partial x_1}{\partial y'} - \frac{(x_1 - x_0)(x' - x_1)}{(x_2 - x_1)^2} \frac{\partial x_2}{\partial y'}, \quad (12)$$

$$\frac{\partial y}{\partial x'} = \frac{y_2 - y'}{y_2 - y_1} \frac{\partial y_0}{\partial x'} - \frac{(y_2 - y_0)(y_2 - y')}{(y_2 - y_1)^2} \frac{\partial y_1}{\partial x'} - \frac{(y_1 - y_0)(y' - y_1)}{(y_2 - y_1)^2} \frac{\partial y_2}{\partial x'}, \quad (13)$$

$$\frac{\partial y}{\partial y'} = \frac{y_2 - y_0}{y_2 - y_1} + \frac{y_2 - y'}{y_2 - y_1} \frac{\partial y_0}{\partial y'} - \frac{(y_2 - y_0)(y_2 - y')}{(y_2 - y_1)^2} \frac{\partial y_1}{\partial y'} - \frac{(y_1 - y_0)(y' - y_1)}{(y_2 - y_1)^2} \frac{\partial y_2}{\partial y'}. \quad (14)$$

Now after having derived the general formulas for mimesis, we turn to the numerical simulations. From formulas (6)-(14), in order to construct our cloak, we only need to know \underline{x}_0 , \underline{x}_1 , \underline{x}_2 and their respective derivatives. The explicit illustrations we have supplied to exemplify the work within this paper have boundaries whose horizontal plane sections are parts of ellipses (sunflower-like petal, cross, circle) or lines (parallelogram, hexagram, triangle).

4 Mimeticism for non-singular cloaks

In Section 3 we presented the theoretical study of the mathematical model underlying our proposal for cloaks with any arbitrary star shaped boundaries cross sections, that perform mimeticism as well as allowing invisibility. In the present section, we illustrate this by examples with piecewise linear or elliptic boundaries and provide their numerical validation.

4.1 Formulas for piecewise linear boundaries

If a piece of the boundary of a star domain D_i is part of a line of the form $y = a_i x + b_i$, then clearly the line through the origin and a point (x', y') intersects this piece of boundary at

$$(x_i, y_i) = \left(\frac{b_i x'}{y' - a_i x'}, \frac{b_i y'}{y' - a_i x'} \right) \quad (15)$$

and hence

$$\frac{\partial x_i}{\partial x'} = \frac{b_i y'}{(y' - a_i x')^2}, \quad \frac{\partial x_i}{\partial y'} = -\frac{b_i x'}{(y' - a_i x')^2}, \quad \frac{\partial y_i}{\partial x'} = \frac{a_i b_i y'}{(y' - a_i x')^2}, \quad \frac{\partial y_i}{\partial y'} = -\frac{a_i b_i x'}{(y' - a_i x')^2}. \quad (16)$$

Of course, in the case where this piece of boundary is a vertical segment with equation $x = c$, then the above intersection is at $(c, c\frac{y'}{x'})$.

4.2 Formulae for piecewise elliptic boundaries

We suppose here that a piece of at least one of our boundary curves S_i is part of a nontrivial ellipse \mathcal{E}_i with equation of the form $(x - a)^2/c_i^2 + (y - b)^2/d_i^2$ where (a, b) is our vantage point. Of course a line $(x(t), y(t)) = (a, b) + t(x' - a, y' - b)$ passing through (a, b) and a different point (x', y') intersects \mathcal{E}_i at two distinct points. For the construction, we need the point (x_i, y_i) of that intersection which is nearer to (x', y') in the sense that $x_i - a$ and $y_i - b$ have the same sign as $x' - a$ and $y' - b$, respectively.

We have

$$\begin{aligned} x_i &= a + \frac{x' - a}{\sqrt{(x' - a)^2/c_i^2 + (y' - b)^2/d_i^2}}, \\ y_i &= b + \frac{y' - b}{\sqrt{(x' - a)^2/c_i^2 + (y' - b)^2/d_i^2}}. \end{aligned} \quad (17)$$

This implies

$$\frac{\partial x_i}{\partial x'} = \frac{1}{\sqrt{\frac{(x'-a)^2}{c_i^2} + \frac{(y'-b)^2}{d_i^2}}} - \frac{(x' - a)^2}{\left(\frac{(x'-a)^2}{c_i^2} + \frac{(y'-b)^2}{d_i^2}\right)^{\frac{3}{2}} c_i^2}, \quad (18)$$

$$\frac{\partial x_i}{\partial y'} = -\frac{(x' - a)(y' - b)}{\left(\frac{(x'-a)^2}{c_i^2} + \frac{(y'-b)^2}{d_i^2}\right)^{\frac{3}{2}} d_i^2}, \quad (19)$$

$$\frac{\partial y_i}{\partial x'} = -\frac{(x' - a)(y' - b)}{\left(\frac{(x'-a)^2}{c_i^2} + \frac{(y'-b)^2}{d_i^2}\right)^{\frac{3}{2}} c_i^2}, \quad (20)$$

$$\frac{\partial y_i}{\partial y'} = \frac{1}{\sqrt{\frac{(x'-a)^2}{c_i^2} + \frac{(y'-b)^2}{d_i^2}}} - \frac{(y' - b)^2}{\left(\frac{(x'-a)^2}{c_i^2} + \frac{(y'-b)^2}{d_i^2}\right)^{\frac{3}{2}} d_i^2}. \quad (21)$$

We can then apply formulae (6)-(14) to build any generalized cloaks involving boundaries of elliptic types, where the center of the ellipse is the vantage point (a, b) .

This has been used in Figure 2 (A), Figure 2 (C), Figures 4 (E) and Figure 9 (B). We note that outside the cloaks in Figure 2 (A) and 2 (C), the scattered field is exactly the same as that of the small disc of radius $r_0 = 0.195$. When the radius r_0 of the disc (that is, when $c_0 = d_0 = r_0$ in equation (17)) tends to zero, the cloaks become singular and the plane matter wave goes unperturbed (invisibility).

4.3 Squaring the circle

In this section, we make a circle have the same (electromagnetic) signature as a virtual small square lying inside its enclosed region and sharing the same centre. In particular, its appearance to an observer will look like that of a square. As above, the transformation

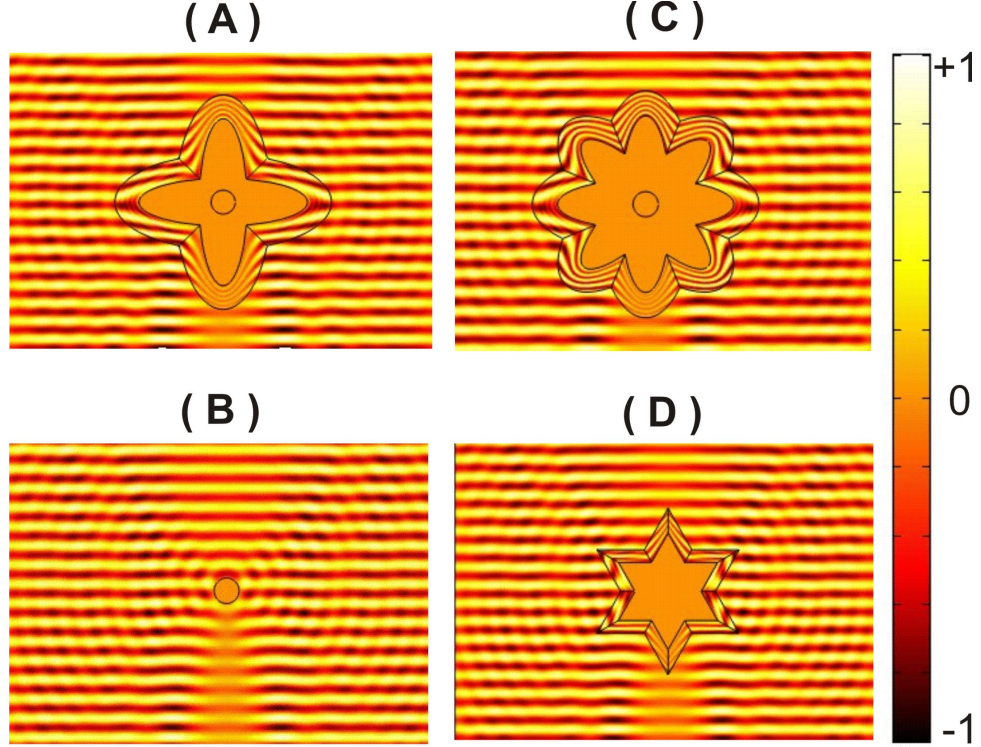


Figure 2: (Color online) A cross-like (A), a sunflower-like (C) and a hexagram (D) all mimicking a circular cylinder (B) of small radius $r_0 = 0.195$, that is $c_0 = d_0 = 0.195$ in equation (17). The inner and outer boundaries of the petals are respectively parts of the ellipses $x^2/0.7^2 + y^2/0.2^2 = 1$ and $x^2/0.9^2 + y^2/0.4^2 = 1$ rotated by angle 0 or $\frac{\pi}{2}$ in (A) or $0, \frac{\pi}{4}, \frac{\pi}{2}$ or $3\pi/4$ in (C). The hexagram (D) is generated from an equilateral triangle with side 1.2 . The energy corresponding to the plane matter wave incident from the top is $E = \sqrt{\omega} = \sqrt{2\pi c/\lambda} = 4.58$, where $\lambda = 0.3$ is the wavelength of a transverse electromagnetic wave in the optics setting with c the celerity of light in vacuum, normalized here to 1. To enhance the scattering, a flat mirror is located under each quantum cloak and obstacle.

will map the region enclosed between the small square and the outer circle into the circular annulus bounded by the inner (cloaking surface) and outer circles, where the sides of the square are mapped to the inner circle and the outer circle stays fixed point wise. To do so, we again use the diagonals of the square to part those regions into sectors. Indeed, the diagonals provide a natural triangulation by dividing the region inclosed inside the square into four sectors. The natural continuation of such a triangulation gives the needed one. In each sector, we apply the same formulas as above, where (x_0, y_0) are obtained from the small square as in Section 4.1 and for both (x_1, y_1) and (x_2, y_2) , we use the same formulas for ellipses in Section 4.2. For the numerical simulation, we use a small square of side $L_0 = 0.2$ and two circles radii $R_1 = c_1 = d_1 = 0.2$, $R_2 = c_2 = d_2 = 0.4$ all centred at $(a, b) = (0, 0)$. So in both the uppermost and lowermost sectors (see Figure 3 (E)) formulas (15) for the square become $(x_0, y_0) = (L_0 \frac{x'}{y'}, L_0)$, whereas in the leftmost and rightmost sectors, we have $(x_0, y_0) = (L_0, L_0 \frac{y'}{x'})$. For all sectors, formulas (17) now read $(x_i, y_i) = (R_i x' (x'^2 + y'^2)^{-\frac{1}{2}}, R_i y' (x'^2 + y'^2)^{-\frac{1}{2}})$, $i = 1, 2$.

The inner boundary of the cloak corresponds to a potential wall (with transformed Neumann boundary conditions, which also hold for infinite conducting or rigid obstacles depending upon the physical context). We report these results in Figure 2 and Figure 4. Some Neumann boundary conditions are set on the ground plane, the inner boundary of the carpet and the rigid obstacle.

4.4 Star shaped cloaks

In this section, we call star shaped a region bounded by a star polygon, such as a pentagram, a hexagram, a decagram, ..., as in [41]. Star shaped regions are particular cases of star regions. The design of star shaped cloaks requires an adapted triangulation of the corresponding region. That is, a triangulation that takes into account the singularities at the vertices of the boundary of the region. So that, each vertex belongs to the edge of some triangle. To the resulting triangles, one applies the same maps as in Section 3. See e.g. Figure 2 (D).

4.5 Finite Element Analysis of the cloak properties

We now turn to specific numerical examples in order to illustrate the efficiency and feasibility of the cloaks we design.

4.5.1 Comparison of backward and forward scattering of isomorphic cloaks

Let us start with a comparison of both backward and forward scattering for the cloaks shown in Figure 2 (D). We report in Figure 3 the amplitude of the matter wave above and below the scatter (cloak and/or obstacle) along the x-axis respectively for $y = 1$ and $y = -1.2$. We note the slight discrepancy between the curves, which is a genuine numerical artefact: we have checked that the finer the mesh of the computational domain, the smaller the discrepancy (which is a good test for the convergence of the numerical package COMSOL Multiphysics). The mesh needs actually be further refined within the heterogeneous anisotropic cloak and the perfectly matched layers compared with the remaining part of the computational domain which is filled with isotropic homogeneous material. We note that the yellow curve (corresponding to the pentagram, see Figure 2 D) is most shifted with respect to the black curve (corresponding to the small obstacle on its own i.e. the benchmark, see Figure 2 B). This can be attributed to the irregular boundary of the cloak as analysed in the case of singular star-shaped cloaks in [41]: we considered around 70000 elements for the mesh in all four computational cases reported in Figure 3 in order to exemplify the numerical inaccuracies. For computations with 100000 elements, the yellow curve is shifted downwards and is nearly superimposed with the black curve. Moreover, the strong asymmetry of the yellow curve in the upper panel of Figure 3 vanishes for 100000 elements. We attribute this numerical effect to the artificial anisotropy induced by the triangular finite element mesh of the pentagram.

4.5.2 Analysis of the material parameters within a cloak

Another interesting point in this paper, is that the metamaterial in our model is non-singular, therefore enabling the implementation of potentially broadband cloaks over a wide range of wavelengths. Moreover, the cloaked objects display a mimesis phenomenon in that, they are designed to acquire any desired quantum or electromagnetic signature.

The result of the numerical exploration of the three eigenvalues $\Lambda_i^{-1}(x, y)$ of the material tensor \mathbf{T}^{-1} , of Figure 4 (E), is reported in Figure 5. First, using Maple software, we have purposely represented those eigenvalues in a wider domain, including the cloaked region, despite the boundary conditions on the inner boundary of cloak. One clearly sees that all of the three eigenvalues take finite values away from 0 even inside the cloak itself. The material tensor \mathbf{T}^{-1} is hence nonsingular. Due to the fourfold symmetric geometry of the cloak (all sectors are obtained by a rotation of any fixed one), we only need to look at those eigenvalues in one sector. We note that $4 > \Lambda_2^{-1} > \Lambda_1^{-1} > 0.2$ in accordance with the fact that the cloak should display a strong anisotropy in the azimuthal direction in order to detour the wave. For a singular cloak Λ_1^{-1} tends to zero on the inner boundary of the cloak, while Λ_2^{-1} tends to infinity.

We also represent the finite element simulation of Λ_3^{-1} , which exemplifies the fourfold symmetry of the isovalues within the circular cloak, a fact reminiscent of the fourfold symmetry of the square which the cloak mimics.

5 Generalized mirage effect and almost trapped states

It is known that a point source located inside the coating of a singular cloak (i.e. a cloak such that $x_0 = y_0 = 0$ in (6)) leads to a mirage effect whereby it seems to radiate from a shifted location in accordance with this geometric transformation [23].

5.1 Shifted quantum dot inside the transformed space

This prompts the question as to whether a similar effect can be observed in non-singular cloaks i.e. when x_0 or y_0 are nonconstant. As it turns out, the physics is now much richer: we can see in Figure 6 that when the source lies inside the coating, it only seems to radiate from a shifted location in accordance with (6), but it is moreover in presence of a small object of sidelength $2x_0$. This can be seen as a generalized mirage effect which opens many new possibilities in optical illusions. Indeed, Nicolet et al. have proposed to extend the concept of mirage effect for point sources located within the heterogeneous anisotropic coating of invisibility cloaks to finite size bodies which scatter waves like bodies shaped by the geometric transform [24]. This is in essence an alternative path to our proposal for mimetism. However, this mirage effect can be further generalized to non-singular for which a finite size body located inside the coating will now create the optical illusion of being another body in presence of some obstacle, which bears some resemblance with Fata Morgana, a mirage which comprises several inverted (upside down) and erect (right side up) images that are stacked on top of one another. Such a mirage occurs because rays of light are bent when they pass through air layers of different temperature. This creates the optical illusion of levitating castles over seas or lakes, as reported by a number of Italian

sailors, hence the name related to Morgana, a fairy central to the Arthurian legend able to make huge objects fly over her lake.

5.2 Field confinement on resonances: Anamorphism fall down

Another intriguing feature of singular cloaks is their potential for light confinement associated with almost trapped states which are eigenfields exponentially decreasing outside the invisibility region. Such modes were described in the context of quantum cloaks by Greenleaf, Kurylev, Lassas and Uhlmann in [20]. These researchers discovered that such modes are associated with energies for which the Dirichlet to Neumann map is not defined i.e. on a discrete set of values. Here, we revisit their paper in light of non-singular quantum cloaks, that is when we consider the blowup of a small region instead of a point. Our findings reported in Figure 7 for a star shaped and a rabbit-like non-singular cloaks mimicking a small disc of radius 0.195 bridge the quantum mechanical spectral problems (panels (a) and (b)) to the scattering problems (panels (c) and (d)) in the following way: we first look for eigenvalues (i.e. quantified energies E) and associated eigenfunctions Ψ of the equation Eq. (4) in the class of square integrable functions on the whole space \mathbb{R}^2 (note that here, as the metric is non singular, there is no need to consider a weighted Sobolev space). Note however that the set continuity conditions on the inner boundary of the cloak, instead of Neumann ones. This provides us with a discrete set of complex eigenfrequencies, with a very small imaginary part (also known as leaky modes in the optical waveguide literature). We neglect this imaginary part and launch a plane wave on the non-singular cloak (whereby the invisibility region is also included within the computational domain as we once again set continuity conditions on the inner boundary of the cloak) at the very frequency given by the spectral problem, see panels (c) and (d). We clearly see that the inside of the cloak hosts a quasi-localized eigenstate whose energy is mostly confined inside a star (panel C) and a rabbit (panel D), both of which actually scatter like a small disc.

6 Generalized super-scattering for negatively refracting non-singular cloaks

In this section, we take some freedom with the one-to-one feature of the previous transforms and allow for space folding. This means that $|x_0| \geq |x_2| \geq |x_1|$ and $|y_0| \geq |y_2| \geq |y_1|$ in (6) while the x_i (resp. the y_i) $i=1,2,3$ all have the same sign, thus making α and β strictly negative real-valued functions. It has been known for a while that space folding allows for the design of perfect lenses, corners and checkerboards [42, 43, 44, 2]. But it is only recently that researchers foresaw the very high-potential of space folding as applied to the design of super-scatterers [45, 46, 47, 48, 49]. We generalize these concepts to mimetism via space folding.

The mapping leading to the super-scatterer is shown in figure 8. We would like to emphasize that here we get not only a magnification of the scattering cross section of an object, in a way similar to what optical space folding does for a cylindrical perfect lens, but we can also importantly change the shape of the object.

We illustrate our proposal with a numerical simulation for a square obstacle surrounded by an anti-cloak in Figure 9(a), which mimics a larger square obstacle, see Figure 9(b). We note that the large field amplitude on the anti-cloak's upper boundary can be attributed to a surface field arising from the physical parameters with opposite signs on the cloak outer boundary (an anisotropic mass density in the context of quantum mechanics and an anisotropic permittivity in the context of optics). It is illuminating here to draw some correspondence with electromagnetic waves, as the anisotropic mass density (resp. permittivity) indeed takes opposite values when we cross the outer boundary of the cloak, and this ensures the existence of a surface matter wave (resp. a surface plasmon polariton) clearly responsible for the large field amplitude (in the transverse electric wave polarization i.e. for a magnetic field parallel orthogonal to the computational plane. We further show an example of a small circular obstacle mimicking a large square obstacle in Figure 9(a) and 9(b). Once again, the large field amplitude on the outer cloak boundary comes from the complementary media inside and outside the cloak. We believe such types of mimetism might have tremendous applications in quantum dot probing, bringing the nano-world a step closer to metamaterials.

7 Conclusion

In this paper, we have proposed some models of generalized cloaks that create some illusion. We focussed here on the Schrödinger equation which is valid in a number of physical situations, such as matter waves in quantum optics. However, the results within this paper can easily be extended to the Helmholtz equation which governs the propagation of acoustic and electromagnetic waves at any frequency. One simply needs to insert the transformation matrix within the shear modulus and density of an elastic bulk (in the case of anti-plane shear waves), the density and compressional modulus of a fluid (in the case of pressure waves), or the permittivity and permeability of a medium (in the case of electromagnetic waves) [11, 12, 13, 14, 15, 16]. In this latter context, this means that in transverse electric polarization (whereby the magnetic field is parallel to the fiber axis), infinite conducting obstacles dressed with these cloaks display an electromagnetic response of other infinite conducting obstacles. In these cloaks, an electric wire could in fact be hiding a larger object near it. Actually, any object could mimic the signature of any other one. For instance, we design a cylindrical cloak so that a circular obstacle behaves like a square obstacle, thereby bringing about one of the oldest enigma of ancient time : squaring the circle! The ordinary singular cloaks then come as a particular case, whereby objects appear as an infinitely small infinite conducting object (of vanishing scattering cross-section) and hence become invisible. On the contrary, such generalized cloaks are described by non-singular permittivity and permeability, even at the cloak's inner surface. We have proposed and discussed some interesting applications in the context of quantum mechanics such as probing nano-objects.

Obviously, one realizes that, when the inner virtual region D_0 responsible for mimetism tends to zero, one recovers the case in [1] where the material properties are no longer bounded, as one of the eigenvalues of the mass density matrix tends to zero whilst another one recedes to infinity, as we approach the inner boundary of the coated region, see also

[21].

In this paper, we have played with optical illusions, trying to be as imaginative as possible in order to exhaust the possible geometric transforms we had at hand in Euclidean spaces (Non-Euclidean cloaking is a scope for more creative thinking [28]). It should be pointed out that while the emphasis of this paper was on quantum waves, corresponding non-singular cloaks in electromagnetism that have an inner boundary which is perfectly electric conducting (PEC) and scatter like a reshaped PEC object, were investigated in [54, 55, 56, 56, 57, 58, 59]. However these works focussed mostly on the reduction of the scattering cross section of a diffracting object, while the present paper explores the mimetism effect whereby an object scatters like another object of any other scattering cross section (and in particular reduced or enhanced ones).

Metamaterials [50] is a vast area with a variety of composites structured on the sub-wavelength scale in order to sculpt the electromagnetic wave trajectories, as experimentally demonstrated at microwave frequencies by a handful of research groups worldwide [51, 52, 53]. Resonant elements within metamaterials are in essence man-made atoms allowing to mimic virtually any electromagnetic response we wish, and this in turn allows us to push the frontiers of photonics towards previously unforeseen areas.

Acknowledgements

AD and SG acknowledge funding from EPSRC grant EPF/027125/1. We authors also wish to thank the anonymous referees for constructive critical comments.

References

References

- [1] Pendry J B, Shurig D and Smith D R 2006 "Controlling electromagnetic fields," *Science* **312** 1780-1782.
- [2] Leonhardt U 2006 "Optical conformal mapping," *Science* **312**, 1777-1780
- [3] Leonhardt U and Philbin T G 2006 "General Relativity in Electrical Engineering," *New J. Phys.* **8**, 247
- [4] Veselago V G 1967 *Usp. Fiz. Nauk* **92** 517-526
- [5] Veselago V G 1968 *Sov. Phys.Usp.* **10** 509-514
- [6] Pendry J B 2000 "Negative refraction makes a perfect lens," *Phys. Rev. Lett.* **86**, 3966-3969.
- [7] Smith D R, Padilla W J, Vier V C, Nemat-Nasser S C and Schultz S 2000 *Phys. Rev. Lett.* **84**, 4184-4187
- [8] Ramakrishna S A 2005 *Rep. Prog. Phys.* **68** 449-521

- [9] Cheianov V V, Fal'ko V, Altshuler B L 2007 *Science* **315**, 1252-1255
- [10] Moreno E, Fernández-Domínguez A I, Cirac J I, García-Vidal F J and Martín-Moreno L 2005 *Phys. Rev. Lett.* **95** 1704061-1704064
- [11] Milton G W, Briane M and Willis J R 2006 *New J. Phys.* **8** 248
- [12] Cummer S A and Schurig D 2007 *New J. Phys.* **9** 45
- [13] Torrent D and Sanchez-Dehesa J 2008 *New J. Phys.* **10** 023004
- [14] Cummer S A, Popa B I, Schurig D, Smith D R, Pendry J, Rahm M and Starr A 2008 *Phys. Rev. Lett.* **100** 024301
- [15] Chen H and Chan C T 2007 *Appl. Phys. Lett.* **91** 183518
- [16] Farhat M, Enoch S, Guenneau S and Movchan A B 2008 "Broadband cylindrical acoustic cloak for linear surface waves in a fluid," *Phys. Rev. Lett.* **101** 134501
- [17] Brun M, Guenneau S and Movchan A B 2009 "Achieving control of in-plane elastic waves," *Appl. Phys. Lett.* **94** 061903
- [18] Farhat M, Guenneau S, Enoch S and Movchan AB 2009 "Cloaking bending waves propagating in thin plates," *Phys. Rev. B* **79** 033102
- [19] Zhang S, Genov D A, Sun C and Zhang X 2008 "Cloaking of matter waves," *Phys. Rev. Lett.* **100** 123002
- [20] Greenleaf A, Kurylev Y, Lassas M, Uhlmann G 2008 *New J. Phys.* **10** 115024
- [21] Kohn R V, Shen H, Vogelius M S and Weinstein M I 2008 "Cloaking via change of variables in electric impedance tomography," *Inverse Problems* **24** 015016
- [22] Greenleaf A, Kurylev Y, Lassas M, Uhlmann G 2007 "Full-wave invisibility of active devices at all frequencies," *Comm. Math. Phys.* **275**(3) 749-789
- [23] Zolla F, Guenneau S, Nicolet A and Pendry J B 2007 "Electromagnetic analysis of cylindrical invisibility cloaks and mirage effect," *Opt. Lett.* **32** 1069-1071
- [24] Nicolet A, Zolla F, and Geuzaine C, "Generalized Cloaking and Optical Polyjuice," arXiv:0909.0848v1.
- [25] Nicorovici N A, McPhedran R C and Milton G W 1994 "Optical and dielectric properties of partially resonant composites," *Phys. Rev. B* **49** 8479-8482
- [26] Torres M, Adrados J P, Montero de Espinosa F R, Garcia-Pablos D, and Fayos J 2000 *Phys. Rev. E* **63** 011204
- [27] Greenleaf A, Lassas M and Uhlmann G 2003 "On nonuniqueness for Calderon's inverse problem," *Math. Res. Lett.* **10** 685-693

- [28] Leonhardt U and Tyc T 2008, "Broadband invisibility by an euclidean cloaking," *Science* **323**(5910), 110-112
- [29] Zhang P, Jin Y, and He S 2008 "Obtaining a nonsingular two-dimensional cloak of complex shape from a perfect three-dimensional cloak," *Appl. Phys. Lett.* **93**, 243502-243504
- [30] Collins P and McGuirk J 2009 "A novel methodology for deriving improved material parameter sets for simplified cylindrical cloaks," *J. Opt. A: Pure Appl. Opt.* **11**, 015104-015111
- [31] Liu R, Ji C, Mock J J, Chin J Y, Cui T J and Smith D R 2008 "Broadband Ground-Plane Cloak," *Science* **323** 366-369
- [32] Li J and Pendry J B 2008 "Hiding under the Carpet: A New Strategy for Cloaking," *Phys. Rev. Lett.* **101** 203901-4
- [33] Pendry J B and Li J 2008 *New J. Phys.* **10** 115032
- [34] Norris A N 2008 *Proc. Roy. Soc. Lond. A* **464** 2411-2434
- [35] Nicorovici N A P, McPhedran R C, Enoch S and Tayeb G 2008 "Finite wavelength cloaking by plasmonic resonance," *New J. Phys.* **10** 115020
- [36] Milton G and Nicorovici NA 2006 "On the cloaking effects associated with anomalous localized resonance," *Proc. Roy. Soc. Lond. A* **462**, 3027
- [37] Alu A and Engheta N 2005 "Achieving Transparency with Plasmonic and Metamaterial Coatings," *Phys. Rev. E* **95**, 016623
- [38] Greenleaf A, Kurylev Y, Lassas M, Uhlmann G 2008 "Electromagnetic wormholes via handlebody constructions," *Comm. Math. Phys.* **281** (2) 369-385
- [39] Gabrielli L H, Cardenas J, Poitras C B and Lipson M 2009 "Silicon nanostructure cloak operating at optical frequencies," *Nature Photonics* **3** 461-463
- [40] Diatta A, Guenneau S, Dupont G and Enoch S 2010 "Broadband cloaking and mirages with flying carpets," *Opt. Express* **18** 11537-11551
- [41] Diatta A, Nicolet A, Guenneau S and Zolla F 2009 "Tessellated and stellated invisibility," *Opt. Express* **17** 13389-13394
- [42] Pendry JB and Ramakrishna SA 2003 "Focussing light with negative refractive index," *J. Phys.: Condens. Matter* **15**, 6345
- [43] Guenneau S, Vutha AC and Ramakrishna SA 2005 "Negative refractive in checkerboards related by mirror-antisymmetry and 3-D corner reflectors," *New J. Phys.* **7**, 164

- [44] Milton GW, Nicorovici NAP, McPhedran RC, Cherednichenko K and Jacob Z 2008 "Solutions in folded geometries, and associated cloaking due to anomalous resonance," *New J. Phys.* **10**, 115021
- [45] Zhang JJ, Luo Y, Chen SH, Huangfu J, Wu BI, Ran L and Jong JA 2009 "Guiding waves through an invisible tunnel," *Opt. Express* **17**, 6203
- [46] Lai Y, Chen H, Zhang ZQ and Chan CT 2009 "Complementary Media Invisibility Cloak that Cloaks Objects at a Distance Outside the Cloaking Shell," *Phys. Rev. Lett.* **102**, 093901
- [47] Lai Y, Ng J, Chen HY, Han DZ, Xiao JJ, Zhang ZQ and Chan CT 2009 "Illusion Optics: The Optical Transformation of an Object into Another Object," *Phys. Rev. Lett.* **102**, 253902
- [48] Ng J, Chen HY and Chan CT 2009 "Metamaterial frequency-selective superabsorber," *Opt. Lett.* **34**, 644
- [49] Wee WH, Pendry JB 2010 "Super phase array," *New J Phys.* **12** 033047
- [50] Zheludev NI 2010 *Science* **328**, 582
- [51] Schurig D, Mock J J, Justice B J, Cummer S A, Pendry J B, Starr A F, Smith D R 2006 "Metamaterial electromagnetic cloak at microwave frequencies," *Science* **314** 977-980
- [52] Kante B, Germain D, de Lustrac A 2009 "Experimental demonstration of a nonmagnetic metamaterial cloak at microwave frequencies," *Phys. Rev. B* **80** 201104
- [53] Tretyakov S, Alitalo P, Luukkonen O, Simovski C 2009 "Broadband electromagnetic cloaking of long cylindrical objects," *Phys. Rev. Lett.* **103** 103905
- [54] Cummer SA, Rupoeng L and Cui TJ 2009 "A rigorous and nonsingular two dimensional cloaking coordinate transformation," *Jour. Appl. Phys.* **105**, 056102
- [55] Hu J, Zhou X and Hu G 2009 "Nonsingular two dimensional cloak of arbitrary shape," *Appl. Phys. Lett* **95**, 011107
- [56] Jiang WX, Cui TJ, Yang XM, Cheng Q, Liu R and Smith DR 2008 "Invisibility cloak without singularity," *Appl. Phys. Lett.* **93**, 194102
- [57] Chen H, Zhang X, Luo X, Ma H and Chan CT 2008 "Reshaping the perfect electrical conductor cylinder arbitrarily," *New J. Phys.* **10**, 113016
- [58] Li C, Yao K and Li F 2008 "Two-dimensional electromagnetic cloaks with non-conformal inner and outer boundaries," *Opt. Express* **16**(23), 19366
- [59] Jiang WX, Ma HF, Cheng Q and Cui TJ 2010 "A class of line transformed cloaks with easily realizable constitutive parameters," *Jour. Appl. Phys.* **107**, 034911

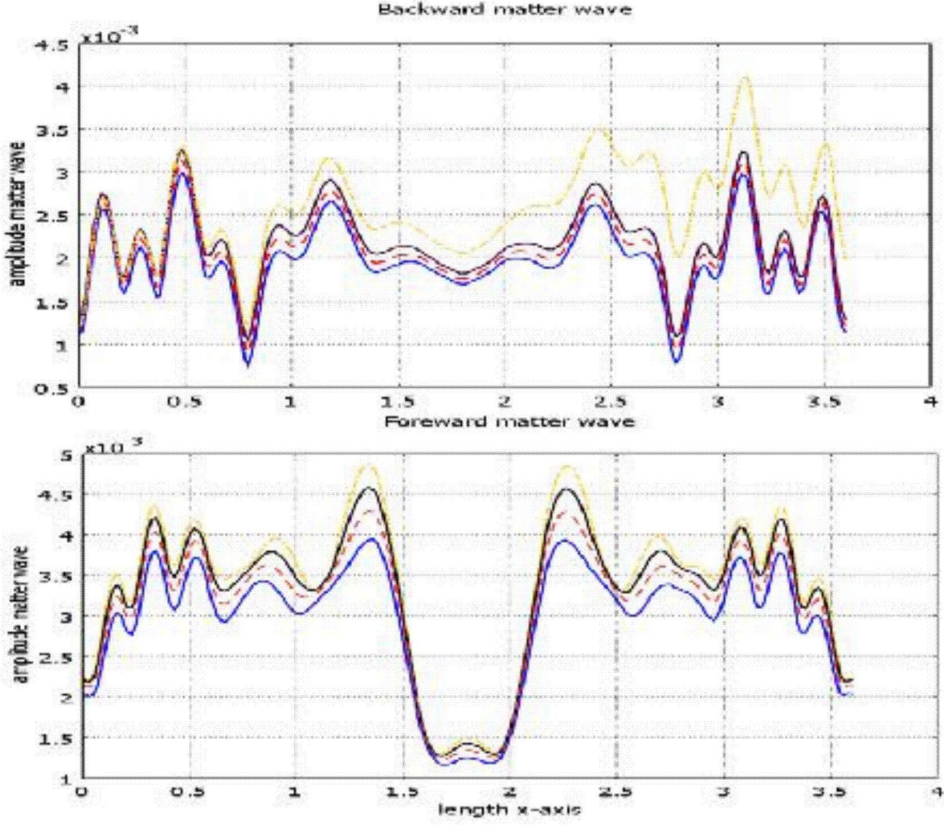


Figure 3: (Color online) Upper panel: Profile of backward matter wave along the x -axis for $y = 1$ for a plane wave incident from the top as in Fig. 2 for a cross-like (solid blue curve, see A), a sunflower-like (dashed red curve, see C), a hexagram (dotted yellow curve, see D) and a circular cylinder of small radius $r_0 = 0.195$ (solid black curve, see B); Lower panel: idem for profile of forward matter wave for $y = -1$; We note the large amplitude of the forward wave, due to the presence of a mirror below each nano scatterer at $y = -1.2$. The slight discrepancy between the curves is attributed to a numerical inaccuracy induced by the highly heterogeneous nature of the cloaks which is further enhanced by the irregularity of the boundary of the starshape cloak (dotted yellow curve, see D). The amplitude of the wave in both panels can be normalized to 1 (dividing throughout by $4.5 \cdot 10^{-3}$ and by $5 \cdot 10^{-3}$ in the upper and lower panels respectively) for comparison with Fig. 2.

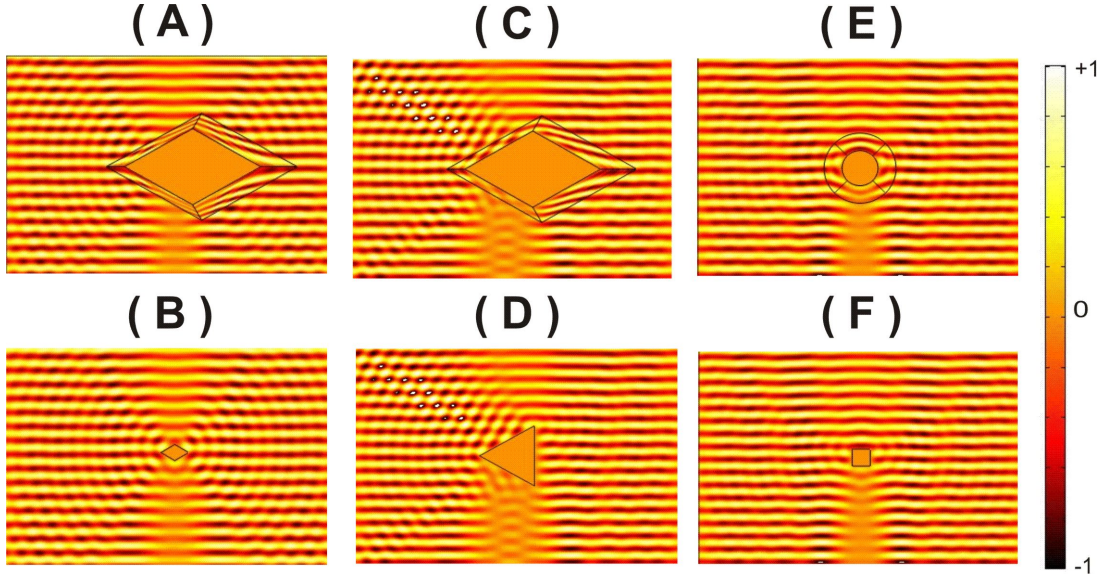


Figure 4: (Color online) Left: A hollow parallelogram cylindrical region (A) scatters any incoming plane wave just like a much smaller solid cylinder (B) of the same nature. In (C) the same hollow parallelogram cylinder is designed to have the same response to waves as the small equilateral triangle (D) with side $\frac{2\sqrt{3}}{5}$. Right, squaring the circle: metamaterials allow to make a circular cylindrical hollow region (inner and outer radii 0.2 and 0.4 respectively) and a small solid square cylinder (of side $L_0 = 0.2$ and having the same center) equivalent, as regards their signatures and the way waves see them. In all these cases, the coated regions not only gain the same electromagnetic signature as any desired other object, but also serve as cloaks with nonsingular material properties, in fact the presence of any types of defects hidden inside them has no effect in the way they scatter waves. The energy corresponding to the plane matter wave incident from the top is $E = \sqrt{\omega} = \sqrt{2\pi c/\lambda} = 4.58$, where $\lambda = 0.3$ is the wavelength of a transverse electromagnetic wave in the optics setting with c the celerity of light in vacuum, normalized here to 1.

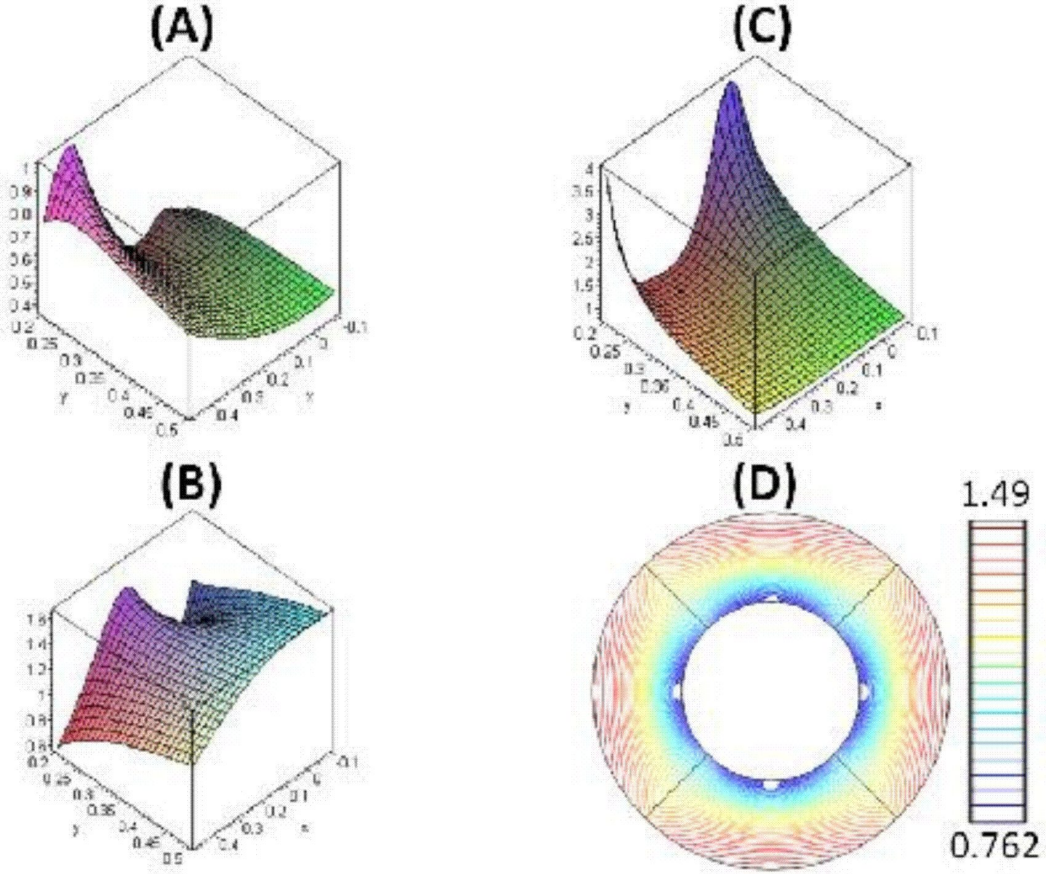


Figure 5: (A)-(C) are illustration of the graphs $\{(x, y, \Lambda_i^{-1})\}$, $i = 1, 2, 3$ of the three eigenvalues Λ_i^{-1} of the material tensor \mathbf{T}^{-1} , in the uppermost sector of Fig. 4 (E): (A) Λ_1^{-1} ; (B) Λ_3^{-1} ; (C) Λ_2^{-1} . We note that, each of all those three surfaces are strictly above the plane $z = 0$ even inside the cloak itself. Because all other sectors of the cloak are obtained by a rotation of the uppermost one, it suffices to study the eigenvalues of \mathbf{T}^{-1} in just one sector. Note that, the above surfaces were drawn using the MAPLE software. In (D) we represent the finite element computation of λ_3 (see B) for all four sectors of Fig. 4 (E) in the COMSOL MULTIPHYSICS package. We note the four-fold symmetry of the isovalues.

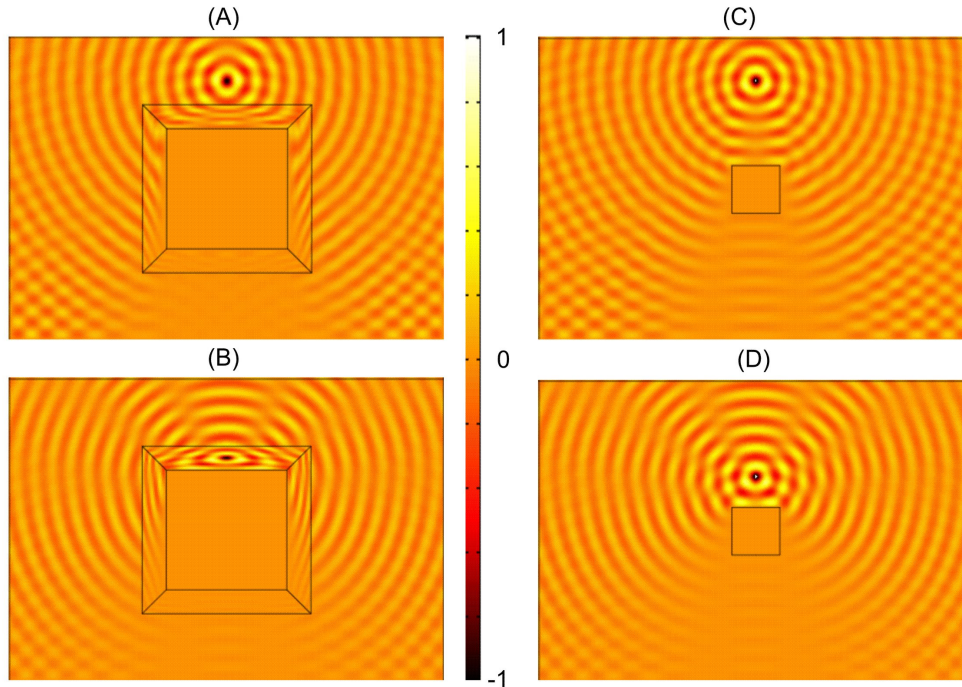


Figure 6: A non-singular cloak with two square boundaries of sidelengths 1 and 1.4 in presence of a quantum dot with energy $E = 4.58$ (resp. an electric current line source of wavelength $\lambda = 0.3$ in the context of transverse electric waves). (A-C) When the source is located a distance 0.2 away from the cloak, it seems to emit as if it would be a distance 0.4 away from a square obstacle of sidelength 0.4. (b-d) When the source is located a distance 0.1 away from the inner boundary of the cloak (i.e. in the middle of the coating), it seems to emit as if it would be a distance 0.25 away from a square obstacle of sidelength 0.4, in accordance with (6) where $x_0 = 0.2$, $x_1 = 0.5$ and $x_2 = 0.7$.

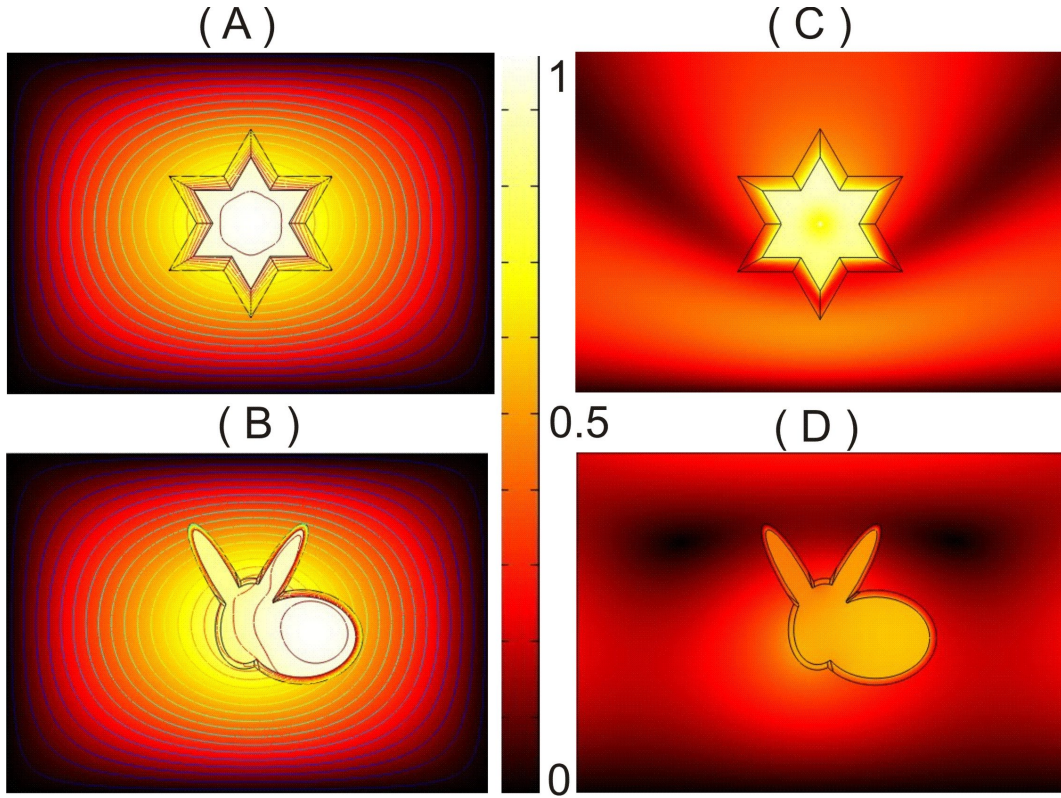


Figure 7: *Left panel: Modulus of the fundamental eigenstates associated with quantified normalized energy $E = \sqrt{\omega} = \sqrt{2\pi c/\lambda} = 1.32$ (resp. a transverse electric plane wave of wavelength $\lambda = 3.6$) for a non-singular cloak shaped as a star (A) and a rabbit (B) both of which mimic a small disc (of normalized radius 0.195, e.g. 195 nanometers) ; Right panel: Matter wave incident from the top on the quantum cloaks with a spatially varying potential V' with compact support (i.e. vanishing outside the cloak) and energy E ; The large amplitude of the field within the cloak is noted.*

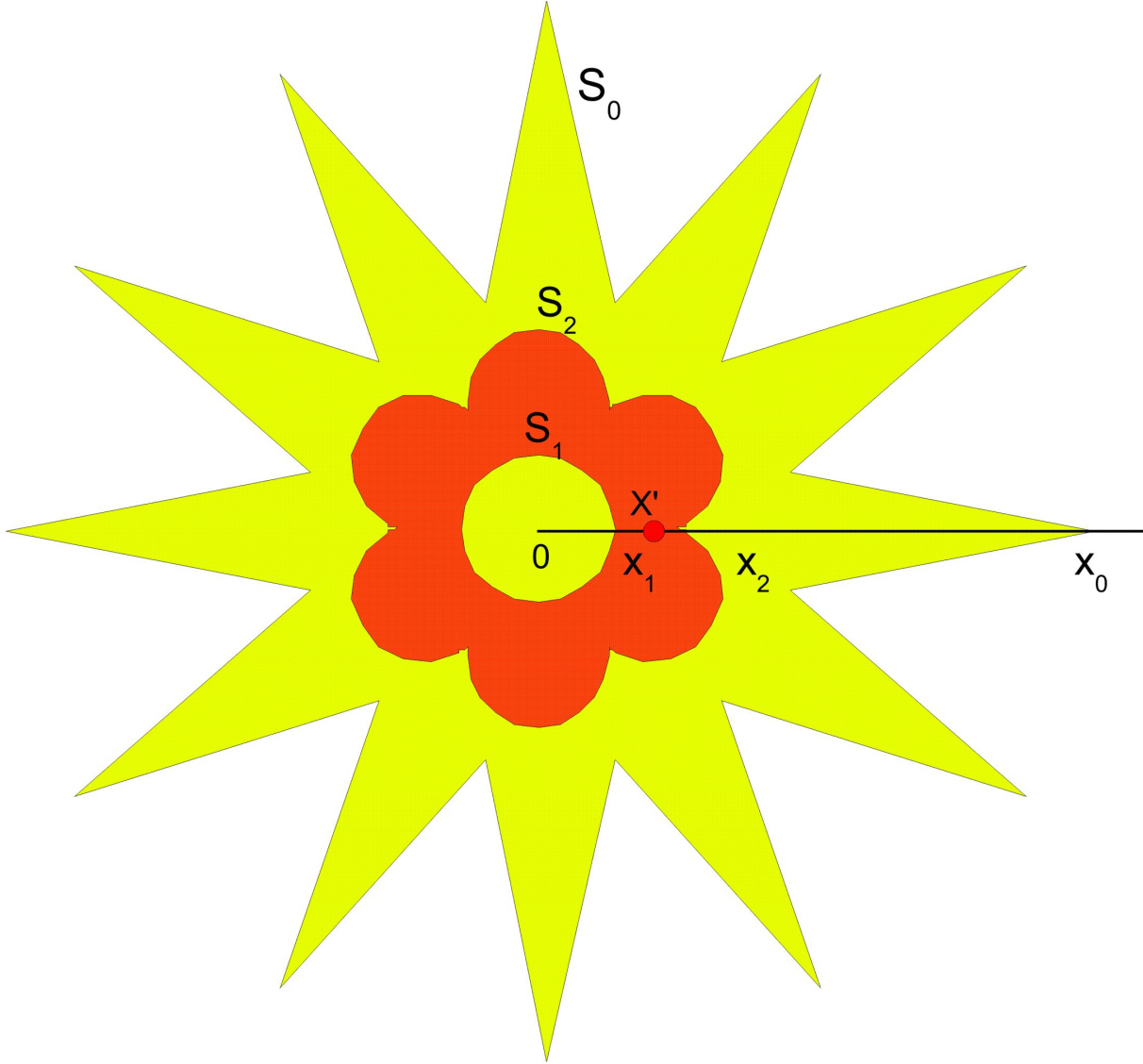


Figure 8: *Construction of a generalized cloak with optical space folding for superscattering effect. The transformation with inverse (6) magnifies the region bounded by the two surfaces S_0 and S_2 into the region bounded by S_1 and S_2 . We note that the transform is no longer an isomorphism. The curvilinear metric inside the carpet (here, an orange flower) is described by the transformation matrix \mathbf{T} , see (7)-(14). Any quantum object located within the region bounded by the surface S_1 scatters matter waves like a larger object bounded by S_0 (here, a yellow star).*

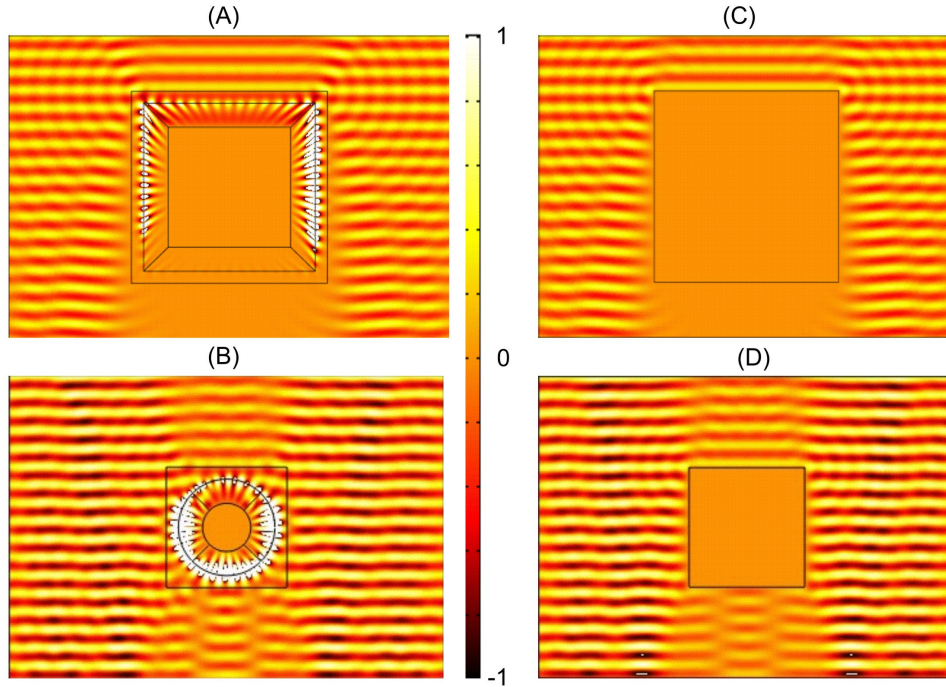


Figure 9: (A-C) Any obstacle surrounded by a square anti-cloak with square boundaries of sidelengths 1 and 1.4, scatters a plane matter wave of energy $E = 4.58$ (resp. a transverse electric plane wave of wavelength $\lambda = 0.3$ in the context of optics) which is coming from the top like a larger square obstacle of sidelength 1.6. (b-d) Any obstacle surrounded by a circular anti-cloak with circular boundaries of radii 0.2 and 0.4 scatters a plane matter wave of energy $E = 4.58$ (resp. a transverse electric plane wave of wavelength $\lambda = 0.3$) which is coming from the top like a larger square obstacle of sidelength 1. The large field amplitude on the upper boundary of the anti-cloak in (A) and (B) is noted. It can be attributed to some kind of surface matter wave (a surface plasmon polariton in the context of optics).